Laser Reflection Intensity and Multi-Layered Laser Range Finders for People Detection

Alexander Carballo, Akihisa Ohya and Shin'ichi Yuta

***Abstract*— Successful detection of people is a basic requirement for a robot to achieve symbiosis in people's daily life. Specifically, a mobile robot designed to follow people needs to keep track of people's position through time, for it defines the robot's position and trajectory.**

In this work we introduce the usage of reflection intensity data of Laser Range Finders (LRF) arranged in multiple layers for people detection. We use supervised learning to train strong classifiers including intensity-based features. Concretely, we propose a calibration method for laser intensity and introduce new intensity-based features for people detection which are combined with range-based features in a strong classifier using supervised learning. We provide experimental results to evaluate the effectiveness of these features.

This work is an step towards of our main research project of developing a social autonomous mobile robot acting as member of a people group.

I. Introduction

Mobile robots are becoming a common part of daily life in tasks like helping the development process in children as well as accompanying elderly people. Such robots are designed to directly interact with people so one important requirement is detection, recognition and tracking of people as well as obstacles in the environment. There are several approaches to separate people from environment objects (people detection) using robot sensory data: by identifying some features from the body, by analyzing motion patterns of some segments in data, by using one type or a fusion of sensors with complementary capabilities, etc.

Vision has been widely considered for people detection and position estimation, using stereo data, color distributions, body parts detection from blobs, pattern matching, etc. [1–6]. However vision-based people detection is still highly sensitive to changes in environment and setup conditions, and people position estimation turns becomes difficult from a mobile platform.

On the other hand, Laser Range Finders (LRF) are an important part of surveillance and people detection and tracking systems, and have important advantages like high accuracy even at large distances, simplicity of usage (little or no calibration/setup), robustness to changes in environment, wider view angles, high scanning rates, small data dimensionality thus less computing resources necessary, and most systems are even safe for human environments. Regarding people detection, human legs have been widely used as features for human detection and tracking [7–11].

Intelligent Robot Laboratory, Graduate School of Systems and Information Engineering, University of Tsukuba, 1-1-1 Tennoudai, Tsukuba City Ibaraki Pref., 305-8573, Japan, +81-29-853-6168. {acs,ohya,yuta}@roboken.esys.tsukuba.ac.jp

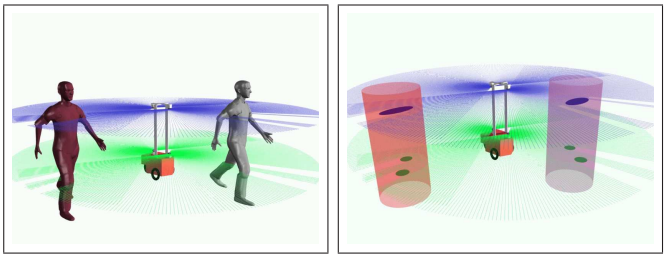

(a) (b)

Fig. 1: People detection approach: (a) two layers of sensors and people around the robot, (b) detection of body parts in each layer (dark elliptical shapes) and people detection (cylinders).

One of the existing problems is how to correctly identify people features (pair of legs) from laser measurements. Arras *et al.* [11] and Zivkovic *et al.* [12] use *AdaBoost* for correct detection people features from LRF segments: using a set of geometrical features from LRF range data (e.g., width, linearity, curvature, etc.), define weak classifiers and then train a strong classifier.

Despite simplicity in LRFs, planar 2D scan data (angle and range) is not enough to understand a 3D world. Occlusions caused by obstacles becomes an important issue; consider for example a person standing behind a desk or a dust bin, while he/she can be still detected using vision, perhaps only the desk will be acquired by the LRF.

To overcome this limitation, we introduced a multi-layered arrangement of LRF sensors for people detection [13], under the concept that the partial occlusion of one layer does not affect detection in the other layers. In our system, sensors are arranged in layers (two sensors per layer) to scan all around the robot; also our system has two layers and data from each layer is processed in parallel. From each layer we find the body parts and combine them together for people detection and position estimation. Fig. 1 represents our layered approach, in Fig. 1(a) the multi-layered LRFs obtain range and intensity data from people possibly having different laser reflection properties, and in Fig. 1(b) using range-based and intensity-based features extract candidate segments for people detection.

Besides range information, LRF sensors can also provide reflection intensity for every laser beam, this is the energy of the reflected laser received in the sensor circuitry. This property has been rarely used, one pioneer work using laser intensity from a mobile robot is attributed to Hancock [14] where a model of laser reflection was proposed, characteriz-

ing the response of the reflected laser depending on surface albedo, roughness, range to target, etc. Recently laser intensity is gaining interest from the research community. Nüchter *et al.* [15, 16] uses range and intensity data together with Haar-like features for object classification. In Montemerlo *et al.* [17] laser intensity is used for extracting road lanes from an autonomous vehicle.

We extend our work by introducing the usage of laser reflection intensity as a novel feature for people detection in our multi-layered system. We propose a simple calibration method of laser reflection intensity for low power LRFs and use laser intensity as part of a segment classifier trained using AdaBoost. To our knowledge no other work considers laser reflection intensity for people detection.

The rest of the paper is structured as follows: Section II briefly describes our multi-layered people detection system. In Section III we explain and propose laser reflection intensity for people detection. Section IV presents experimental results of our people detection method and finally, conclusions and future works are left for Section V.

II. System Overview

Our main research problem aims to develop a companion robot with the particular objective to study the relationship of an autonomous mobile robot as a member of a group of multiple people in complex environments like public areas, where the robot is to move and behave like another member of the group.

As presented in our previous work [13], the current implementation of our system has two layers of LRF sensors: the top layer located about 110cm and the bottom layer about 40cm from the ground. Each layer has two sensors facing opposite directions to produce a 360^o representation of robot's surroundings. From every layer, LRF data is first divided into segments S_i, from each segment we compute a set of n features $\mathbf{h}(S_i) \in \mathbb{R}^n$ which help classifying segments as body parts (chests or legs).

Based on Arras *et al.* [11], we defined the following list of features from every segment:

1) **Number of points** (N) of the segment.
2) **Width** (w), longest side of the segment's bounding box $w = \max(W, H)$, with W and H the sides of the box.
3) **Size ratio** (ℓ), ratio of the sides of the segment's bounding box $\ell = \frac{\max(W,H)}{\min(W,H)}$.
4) **Radius** (R), from the best fitting circle.
5) **Boundary length** (bl), average distance between points $bl = \frac{1}{N}\sum_{i=1}^{N-1} D(f_i, f_{i+1})$.
6) **Boundary regularity** (br): standard deviation of the boundary length.
7) **Mean curvature** ($\bar{\kappa}$): mean of the curvatures κ_i from the triangle $\triangle f_{i-1} f_i f_{i+1}$, every three points, $\kappa_i = \frac{4A}{D(f_{i-i}, f_i) D(f_i, f_{i+1}) D(f_{i-1}, f_{i+1})}$, A triangle's area.
8) **Normalized number of points** ($\widehat{N}$), the ratio of the actual number of points and the maximum expected number of points at a given range, $\widehat{N} = \frac{2N\rho \tan(\vartheta/2)}{w_{\max}}$, where ρ is the range to the segment center, ϑ is the angular resolution of the sensor and $w_{\max}$ is the maximum expected width of a person.

Also based on Arras *et al.* [11], we used the AdaBoost algorithm to train a strong classifier $\mathcal{H}$ to detect body parts. We defined a set of m labeled training examples by manual labeling. The final strong classifier $\mathcal{H}$ is:

$$\mathcal{H}(S) = \text{sign}\left(\sum_{t=1}^{T} \omega_t g_t(S)\right) \tag{1}$$

The weak classifier function $g_t(S)$ evaluates the t-th feature $h_t(S)$ as follows:

$$g_t(S) = \begin{cases} +1 & \text{if } s_t h_t(S) < s_t \theta_t, \\ -1 & \text{otherwise.} \end{cases} \tag{2}$$

AdaBoost allows learning the parameters: ω_t which is a weight applied to the weak classifier g_t, θ_t the threshold for the feature h_t and $s_t \in \{+1, -1\}$ the sign defining the direction of the inequality; T is the number of weak classifiers.

Feature classification is done separately per layer, therefore we trained two separated strong classifiers, $\mathcal{H}_{\text{top}}$ for chest segments in the top layer and $\mathcal{H}_{\text{bottom}}$ for legs in the bottom layer. The classification step concludes by labeling segments as *candidate* using the output from both $\mathcal{H}_{\text{top}}$ and $\mathcal{H}_{\text{bottom}}$, according to the segment's layer.

In [13] we proposed a method to combine candidate segments from both layers by defining a search radius of λ_s. The chest segment is projected into the bottom layer to search for the corresponding leg(s), if the distance from the chest segment to the leg segment is less than λ_s we successfully detect a person.

Regarding people position, for every person $\mathcal{P}_i$ we use the center of the chest segment as the expected position $\mu_i = \begin{bmatrix} x_i & y_i \end{bmatrix}^\mathsf{T}$ of the person. In a data association step, newly detected person $\widehat{\mathcal{P}}_i^t$ is associated with an already known person $\mathcal{P}_k^{t-1}$ from a list $\boldsymbol{\mathcal{P}}^{t-1}$ from time $t-1$. For every new person $\widehat{\mathcal{P}}_i^t$ we find the closest $\mathcal{P}_k^{t-1}$ using the Mahalanobis distance $d(i,k)$ with the estimated positions μ_i^t for $\widehat{\mathcal{P}}_i^t$ and μ_k^{t-1} for $\mathcal{P}_k^{t-1}$. If the minimum $d(i,k)$ is smaller than some $d_{max} = \lambda_s$ then $\widehat{\mathcal{P}}_i^t$ and $\mathcal{P}_k^{t-1}$ are associated in the new list $\boldsymbol{\mathcal{P}}^t$, else $\widehat{\mathcal{P}}_i^t$ is regarded as a new person included $\boldsymbol{\mathcal{P}}^t$. Tolerance to occlusions is achieved by relaxing this association to allow single body parts, this is candidate segments for which no corresponding part could be found in the opposite layer, to become associated to known persons (partial associations).

III. Laser Intensity for People Detection

Reflected intensity of laser depends upon several properties:

- Color
- Material and Roughness
- Distance to the source (sensor)
- Angle of incidence
- Power of the laser beam, wavelength, etc.

Colors and materials of objects in indoor environments (walls, doors, windows, metallic objects, etc.) are usually

different from clothes. The intensity of the reflected laser beam is different from environment objects and from people, and can be used for separation of people from environment objects and even some form of identification could also be achieved with a proper laser characterization [14].

A. Calibration of Laser Intensity

The *URG-04LX* presents a characteristic *sigmoid* curve for intensity decay with range. Based on the *Gompertz* growth function[18], we defined the decay function for intensity as a function of range as:

$$\mathcal{F}_\rho(i) = a\left(1 - \exp(b\exp\left(c\rho_i\right))\right) \tag{3}$$

where ρ_i is the i-th beam's range, a is the upper asymptote, b and c (both negative numbers) are decay parameters. Non-linear least squares was used to find the parameters (a, b, c). This characteristic sigmoid form can be clearly appreciated in

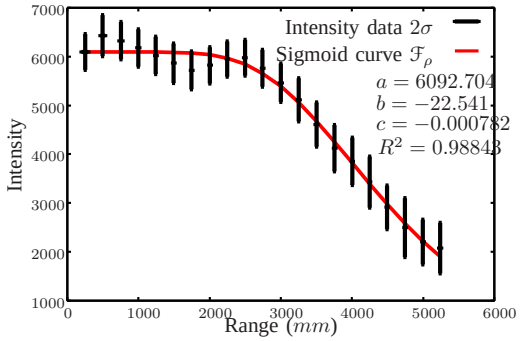

Fig. 2: Intensity decay by varying distance for the URG-04LX sensor.

Fig. 2. This curve was obtained from a white target ($90g/m^2$, $0.13mm$ white bond paper) with an angle of incidence close to zero (vertical error bars for two standard deviations 2σ, data was collected during $60s$ at each range), the continuous curve corresponds to the function $\mathcal{F}_\rho$ fitted to white paper data with the given parameters.

From a practical point of view, our *URG-04LX* sensor is designed for small areas (maximum range is 5.6m) so its laser is emitted with very little power, specially when compared with LRF sensors like the SICK *LMS200* for ranges up to 80m. The intensity value I for one object will be different depending on the range to that object, limiting the applications of laser intensity. Therefore some form of normalization is sought so that an object can be detected for its particular reflectivity (e.g., color, material, etc.) regardless of the range.

We consider the expression in Eq. 3 as the maximum expected intensity for some distance, then we calibrate the actual intensity value I_i of the i-th laser beam as:

$$\mathcal{I}(i) = \frac{I_i}{\mathcal{F}_\rho(i)} \tag{4}$$

This expression reduces the sigmoid decay effect with range to the object. However the laser reflected intensity still depends on several other properties such as indicated above, which will be considered in a future work.

B. Laser Intensity Features

Once laser intensity is calibrated, the—calibrated—intensity mean $\mu_\mathcal{I}$ and variance $\sigma^2_\mathcal{I}$ from Eq. 4, calculated for every segment, serve to measure the intensity distribution of an object. We also consider how intensity changes between consecutive points p_i^j and p_{i+1}^j inside a segment j using differences of intensity:

$$\mathcal{D}_j(i) = \mathcal{I}(p_i^j) - \mathcal{I}(p_{i+1}^j) \tag{5}$$

The *variance of intensity differences* $\sigma^2_\mathcal{D}$ also serves to measure the *intensity uniformity* of an object: if the object has uniform reflection (i.e., a smooth surface with a single color) then $\sigma^2_\mathcal{D}$ will be small as the differences tend to be small. This *variance of intensity differences* is:

$$\sigma^2_{\mathcal{D}_j} = \frac{1}{N}\sum_{i=1}^{N}\left(\mathcal{D}_j(i) - \mu_{\mathcal{D}_j}\right)^2 \tag{6}$$

where $\mu_{\mathcal{D}_j}$ is the average of such difference over all the points in segment j.

To evaluate the effect of laser reflection intensity for people detection, we defined three experiment scenarios using actual range and intensity data from people and environment objects. The experiments involve two people moving in a narrow corridor and are wearing different colors (in this case dark gray and beige shirts). Fig. 3 presents scan data for these three cases and their respective graphs of differences of intensity $\mathcal{D}_j$, detected people are represented in the figures as cylinders. Case A in Fig. 3(a) shows persons P0 and P1 separated and correctly detected (marked here by cylinders). Case B in Fig. 3(b) shows two persons standing very close and their LRF segments cannot be separated (segment 1(t)). Finally, Case C in Fig. 3(c) shows two persons and one is leaning against a wall (segment 2(t)).

The right column of Fig. 3 shows the graph of differences of calibrated intensity $\mathcal{D}$ for all the segments in the top layer, including their respective variances ($\sigma^2_\mathcal{D}$). Other detailed information of these segments appears in Table I. One thing we can observe is that segments corresponding only to walls (segments 0(t) and 3(t) in Fig. 3(a), segments 0(t) and 2(t) in Fig. 3(b) and segment 0(t) in Fig. 3(c)) have smaller $\sigma^2_\mathcal{D}$ since their reflective property is quite uniform.

TABLE I: Segment parameters (top layer)

Case	Seg.	$\mu_\mathcal{D}$	$\sigma^2_\mathcal{D}$	ℓ	w
A	0	0.000052	0.001067	121.219	5767.907
	1	0.011512	**0.008663**	3.789	427.895
	2	0.018666	**0.022276**	2.667	469.681
	3	0.000736	0.000444	116.857	5513.667
B	0	0.000107	0.000921	111.213	5746.118
	1	-0.005758	**0.015570**	5.467	922.348
	2	0.000091	0.000474	113.436	5893.558
C	0	0.000085	0.000962	110.988	5073.084
	1	-0.023403	**0.025974**	2.909	449.623
	2	0.022062	**0.029477**	8.759	4912.623

In Table I we include LRF range and intensity information for each case (in this implementation we consider only the top layer), segments corresponding to people (both separated

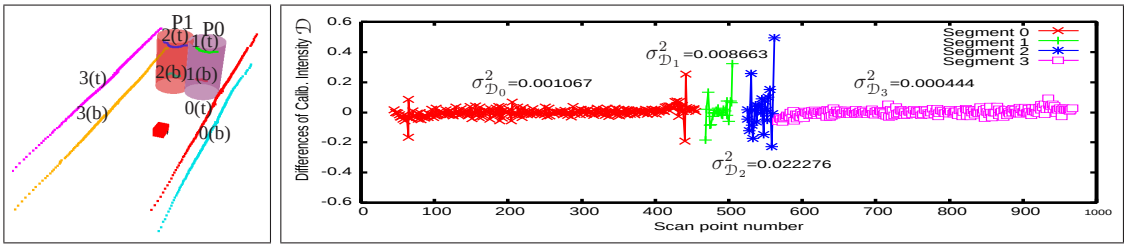

(a) Two persons (Case A)

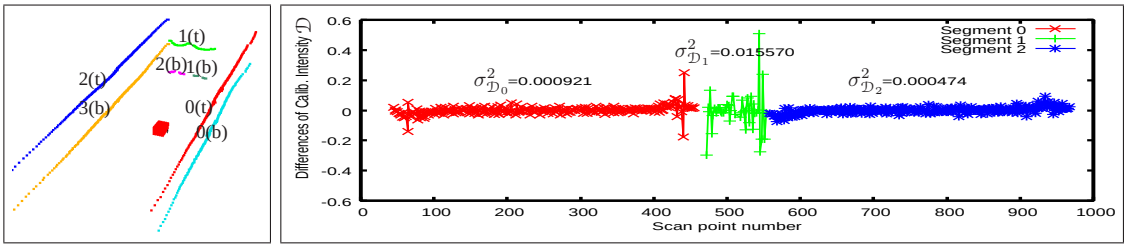

(b) Two persons very close (Case B)

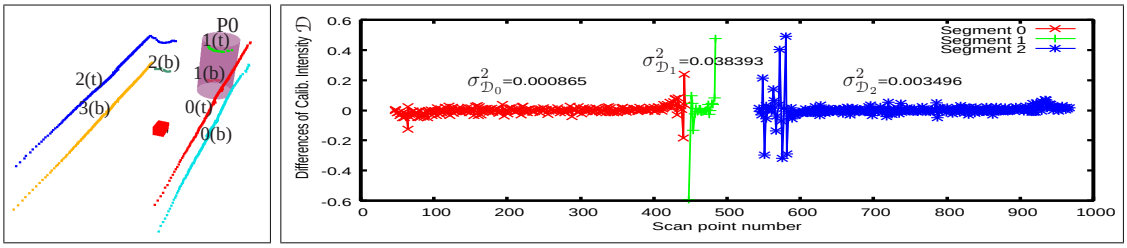

(c) A person against a wall (Case C)

Fig. 3: Scan segments for three different cases: (a) two persons separated, (b) two persons very close, (c) a person very close to a wall, "(t)" stands for top and "(b)" for bottom.

and close) are highlighted with bold characters. From range-based features, segments from people have a small size ratio ℓ(which also serve as a measure of linearity) and also small width w value. In the case of merged segments (two different objects very close forming one segment) separation of the individual objects is difficult using only range-based features. However we can observe that the variance $\sigma^2_{\mathcal{D}}$ is large for all the scan segments from people, even the case of a person segment is merged with the wall segment (segment 2 from Case C).

We extended the list in Section II with new intensity-based features for people detection. Once more, we used AdaBoost to train two new strong classifiers ($\mathcal{H}^+_{\text{top}}$ and $\mathcal{H}^+_{\text{bottom}}$) including these new intensity-based features.

9) **Average intensity** ($\mu_{\mathcal{I}}$), the average of the calibrated intensity.
10) **Intensity variation** ($\sigma^2_{\mathcal{I}}$), the variance of calibrated intensity.
11) **Average difference of intensity** ($\mu_{\mathcal{D}}$), the average of the differences of calibrated intensity.
12) **Intensity uniformity** ($\sigma^2_{\mathcal{D}}$), the variance of differences of calibrated intensity.

IV. Experimental Results

We use four Hokuyo *URG-04LX* range scanner sensors, which use a near-infrared (NIR) solid-state laser with $785nm$ wavelength. For data processing and robot control we use a notebook computer with an Intel Core 2 Duo processor at $1.83GHz$, $2GB$ of RAM, running Linux (kernel 2.6.35) as operating system. The processing time from sensor fusion to people detection was in average $52ms$, fast enough given the sensor's scanning speed of $100ms$.

Normally, *URG-04LX*'s range data consists in 682 points circularly ordered from right to left and with an angular resolution of 0.36^o. However, in order to obtain range and intensity simultaneously from the sensor, the number of scan points decreases to one half (341 points) and the angular resolution becomes 0.72^o. LRF data was obtained after warming up the sensors for about $60mins$ to avoid range and intensity drifting due to changes in internal sensor temperature, in this work we do not attempt temperature calibration of laser intensity.

We evaluated our detection method in 3 different environments and conditions for a robot and a group of people:

- A cluttered office area ("Office")
- Several people around the robot ("Crowd")
- Robot with people in narrow hallways ("Hallway")

In left column of Fig. 4 we show pictures of the different

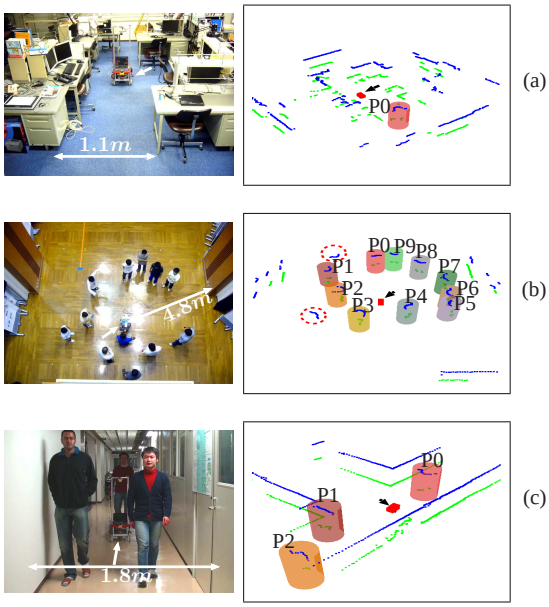

Fig. 4: Scenarios and results of three different experiments: "Office" test (a) detected person $P0$; "Crowd" test (b) 10 out of 12 persons detected $P0$ to $P9$ (missing persons marked with circles); "Hallway" test (c) detected people are $P0$, $P1$ and $P2$.

scenarios, the robot position is marked with an arrow. The "Office" test in Fig. 4(a) consists in an office area with bookshelves, desks, chairs and dust bins, with heavy cluttering at both top and bottom layers, one person moves around in front of the robot and behind desks. The "Crowd" test in Fig. 4(b) is a wide environment with no cluttering but includes 12 people of diverse sizes and clothes colors moving around the robot. Finally the "Hallway" test in Fig. 4(c) consists in long and narrow passages with cluttering (shoe-racks, umbrella stands, etc.), where the robot moved inside a group of three persons (operated by remote control). In the right column of Fig. 4 we include snapshots of our detection system (darker points correspond to top layer). In every figure detected persons are labeled as P_i and marked with a cylinder.

A. People Detection from Range-based Features

We include detection rates for every experimental case in Table II, scan segments were manually labeled into person or not-person to establish the ground truth. The "Office" test consisted in 368 multi-layer observations (parallel scans) and a total of 23003 segments, the true detection rate was 83.3%, false positive rate was 12.5% due to misclassification of books in top layer and chairs in the bottom layer, and a false negative rate of 4.2% due a person walking behind desks and not being detected immediately after reappearing. The "Crowd" test consisted in 164 observations (6351 segments) for a true detection rate of 85.4%, complete occlusions (people walking behind people and very close) is largely responsible for the 11.6% false negative rate. Finally the "Hallway" test had 1238 observations (27662 segments) for a detection rate of 77.4%, although this environment has relatively little cluttering, several objects and particularly some glass structures which were misclassified as people (9.4% false positive rate) and people walking too close to the walls largely accounts for the 13.2% false negative rate.

TABLE II: Multi-Layer detection rates

	True Detection	False Positive	False Negative
Office	**83.3%**	12.5%	4.2%
Crowd	**85.4%**	3.0%	11.6%
Hallway	**77.4%**	9.4%	13.2%

B. People Detection from Intensity-based Features

Using same scan data from the previous test scenarios, we repeated the detection evaluation but this time using laser reflection intensity features and the strong classifiers $\mathcal{H}^{+}_{\text{top}}$ and $\mathcal{H}^{+}_{\text{bottom}}$. Detection results for every case are summarized in Table III. In the "Office" test the number of false negatives did not changed much due to the same problem explained above, but the true detection rate increased 7.8%. In the other tests, higher decrease in false negative rates was achieved: in the "Crowd" test false negatives reduced 4.9% (true rate increased 5.3%) and for the "Hallway" test the false negative rate decreased 8.1% (true rate increased 10.8%). Intensity-based features contributed importantly to to reduce misdetections.

TABLE III: Multi-Layer detection rates using intensity

	True Detection	False Positive	False Negative
Office	**91.1%**	4.7%	4.2%
Crowd	**90.7%**	2.6%	6.7%
Hallway	**88.2%**	6.7%	5.1%

V. Conclusions and Future Works

In this work, we presented a multi-layered people detection system to simultaneously detect different body parts from people around a mobile robot. Detected body parts are combined using a search method and then the position of every person is computed using a simple data association method was used to improve position estimations. By allowing partial associations simple occlusion tolerance was achieved.

The sensor used has a fast intensity decay with range, a method for intensity calibration was introduced. With the range-based features and the new intensity-based features we trained two strong classifiers to detect body parts.

As future works, we plan use our detection method in more realistic environments like public areas and outdoor areas to evaluate its effectiveness, particularly of the intensity-based features. Separation of merged LRF segments of very close objects from their different reflection properties will be also considered. Other future steps of this research include adaptation to changes in group formation, obstacle avoidance inside the people group and from external objects, and assigning different roles (lead, middle, tail) inside the group.

References

[1] C. Schlegel, J. Illmann, H. Jaberg, M. Schuster, and R. Wörz, "Vision based person tracking with a mobile robot," in *Proceedings 9th British Machine Vision Conference*, 1998, pp. 418–427.

[2] Y. Nakauchi and R. Simmons, "Social behavioral robot that stands in line," in *Proceedings of the IEEE International Conference on Systems, Man, and Cybernetics (SMC)*, Tokyo, Japan, October 1999, pp. 993–998.

[3] C. L. Zitnick and T. Kanade, "A cooperative algorithm for stereo matching and occlusion detection," *IEEE Transactions on Pattern Analysis and Machine Intelligence*, vol. 22, no. 7, pp. 675–684, 2000.

[4] D. Beymer and K. Konolige, "Tracking people from a mobile platform," in *Proceedings of the International Joint Conference on Artificial Intelligence*, 2001.

[5] S. Bahadori, G. Grisetti, L. Iocchi, R. Leone, and D. Nardi, "Real-time tracking of multiple people through stereo vision," in *Proceedings of IEE International Workshop on Intelligent Environments*, 2005.

[6] R. Muñoz-Salinas, E. Aguirre, and M. García-Silvente, "People detection and tracking using stereo vision and color," *Journal of Image Vision and Computing*, vol. 25, no. 6, pp. 995–1007, 2007.

[7] A. Fod, A. Howard, and M. J. Matarić, "Laser-based people tracking," in *IEEE International Conference on Robotics and Automation (ICRA)*, Washington D.C., May 2002, pp. 3024–3029.

[8] M. Montemerlo, S. Thrun, and W. Whittaker, "Conditional particle filters for simultaneous mobile robot localization and people-tracking," in *IEEE International Conference on Robotics and Automation (ICRA)*, Washington, D.C., May 2002, pp. 695–701.

[9] J. H. Lee, T. Tsubouchi, K. Yamamoto, and S. Egawa, "People tracking using a robot in motion with laser range finder," in *IEEE/RSJ International Conference on Intelligent Robots and Systems (IROS)*, Beijing, China, October 2006, pp. 2936–2942.

[10] H. Zhao, Y. Chen, X. Shao, K. Katabira, and R. Shibasaki, "Monitoring a populated environment using single-row laser range scanners from a mobile platform," in *IEEE International Conference on Robotics and Automation (ICRA)*, Roma, Italy, April 2007, pp. 4739–4745.

[11] K. O. Arras, Ó. Martínez Mozos, and W. Burgard, "Using boosted features for the detection of people in 2d range data," in *IEEE International Conference on Robotics and Automation (ICRA)*, Roma, Italy, April 2007, pp. 3402–3407.

[12] Z. Zivkovic and B. Kröse, "Part based people detection using 2d range data and images," in *IEEE International Conference on Intelligent Robots and Systems (IROS)*, San Diego CA, October 2007, pp. 214–219.

[13] A. Carballo, A. Ohya, and S. Yuta, "Fusion of double layered multiple laser range finders for people detection from a mobile robot," in *IEEE International Conference on Multisensor Fusion and Integration for Intelligent Systems (MFI)*, Seoul, Korea, August 2008, pp. 677–682.

[14] J. Hancock, "Laser intensity-based obstacle detection and tracking," Ph.D. dissertation, Robotics Institute, Carnegie Mellon University, Pittsburgh, PA, January 1999.

[15] H. Surmann, A. Nüchter, and J. Hertzberg, "An autonomous mobile robot with a 3d laser range finder for 3d exploration and digitalization of indoor environments," *Robotics and Autonomous Systems*, vol. 45, no. 3-4, pp. 181–198, 2003.

[16] A. Nüchter, H. Surmann, and J. Hertzberg, "Automatic classification of objects in 3d laser range scans," in *8th Conference on Intelligent Autonomous Systems (IAS)*, Amsterdam, Netherlands, March 2005, pp. 963–970.

[17] M. Montemerlo, J. Becker, S. Bhat, H. Dahlkamp, D. Dolgov, S. Ettinger, D. Haehnel, T. Hilden, G. Hoffmann, B. Huhnke, D. Johnston, S. Klumpp, D. Langer, A. Levandowski, J. Levinson, J. Marcil, D. Orenstein, J. Paefgen, I. Penny, A. Petrovskaya, M. Pflueger, G. Stanek, D. Stavens, A. Vogt, and S. Thrun, "Junior: The Stanford Entry in the Urban Challenge," *Journal of Field Robotics*, vol. 25, no. 9, 2008.

[18] D. Jukić, G. Kralik, and R. Scitovski, "Least-squares fitting gompertz curve," *Journal of Computational and Applied Mathematics*, vol. 169, pp. 359–375, 2004.